Characterization of Intercalated Iron(III) Nanoparticles and Oxidative Adsorption of Arsenite on Them Monitored by X-ray Absorption Fine Structure Combined with Fluorescence Spectrometry

Yasuo Izumi,*,† Dilshad Masih,† Ken-ichi Aika,† and Yoshimi Seida‡

Interdisciplinary Graduate School of Science and Engineering, Tokyo Institute of Technology, 4259-G1-16, Nagatsuta, Midori-ku, Yokohama 226-8502, and Institute of Research and Innovation, 1201 Takada, Kashiwa 277-0861, Japan

Received: June 5, 2004; In Final Form: November 9, 2004

This paper first deals with the screening and optimization of Fe^{III}-based adsorbents for arsenic adsorption from 0.2 to 16 ppm test solutions of arsenite/arsenate. The best adsorption capacity has been reported on α-FeO(OH) on an adsorbent weight basis. Better results were found on intercalated Fe-montmorillonites for arsenite adsorption below the equilibrium dissolved As concentration of 310 ppb and for arsenate adsorption in all of the concentrations studied. Next, the speciation of As adsorbed was performed by As K-edge x-ray absorption fine structure (XAFS) combined with high-energy-resolution fluorescence spectrometry. Major oxidative adsorption of arsenite was observed on Fe-montmorillonite from the 0.2−16 ppm test solutions. The reasons for the higher capacity of arsenic adsorption and oxidative adsorption of arsenite on Fe-montmorillonite are discussed.

Introduction

Regulations concerning the concentration of arsenic in public water supplies are becoming severe, at 10 ppb, due to the high carcinogenic risk.[1,2] The removal of As from water by the adsorption method is economically advantageous compared to methods using membrane, ion exchange, or reverse osmosis. For the removal of trace amounts of As in drinking water, we screened Fe^{III}-based materials to optimize the greatest adsorption capacity of arsenite/arsenate.[3] The adsorbents included α-FeO(OH) with specific surface area (SA) of 16−54 $m^2\ g^{-1}$ and intercalated FeO(OH) nanoparticles between montmorillonites. In this paper, the responsible structure was studied for the optimized adsorbent by using Fe K-edge EXAFS (extended X-ray absorption fine structure).

The understanding of the removal mechanism from low concentrations of metals in water is important to feed back to the investigation of adsorbents. Recently, the switching of the removal mechanism of Pb^{2+} on $Mg_6Fe_2(OH)_{16}(CO_3)\cdot 3H_2O$ was reported. By the observations using XAFS combined with fluorescence spectrometry, it was found that coagulation took place from 1.0 ppm test solutions of Pb^{2+}, in contrast to the observation that the surface ion exchange occurred with surface hydroxyl groups from 0.1 ppm test solutions of Pb^{2+}.[4,5] In comparison to conventional XAFS, the combination of XAFS with high-energy-resolution fluorescence spectrometry enabled one to observe low concentrations of Pb with far better signal/background (*S/B*) ratios in the presence of high concentrations of Fe in samples.

Furthermore, better energy resolution of XANES (X-ray absorption near-edge structure) spectra is required to quantify each oxidation state for arsenic (As^{III} and As^{V}). Valence information is crucial to the study of arsenic removal, because arsenite is particularly toxic.[1,2] In this study, XAFS combined with fluorescence spectrometry was applied to As adsorbed on the adsorbent optimized among the Fe^{III}-based materials.

Experimental Section

Preparation of Fe-Montmorillonites. A quantity (1.1−7.2 mL) of a 0.43 M Fe^{III} nitrate solution was mixed at 290 K for 2 h with 200 mL of a 0.5 wt % Na-montmorillonite (Kunipia F; $Na_{1.5}Ca_{0.096}Al_{5.1}Mg_{1.0}Fe_{0.33}Si_{12}O_{27.6}(OH)_{6.4}$) suspended in distilled water. Na-montmorillonite was used as received. The primary particle size of Na-montmorillonite was 0.1−1.0 μm. A 0.75 M sodium hydroxide solution was added dropwise to the above mixture until the molar ratio of Fe^{3+} added and hydroxide reached 1:2.

The mixture was stirred at 290 K for 12 h. It was filtered and washed with distilled water until the pH of the filtrate became higher than 6.5. The resultant powder was dried at 313 K for 72 h. Intercalated Fe^{III}-based materials prepared by this route are called Fe-montmorillonites.

Samples were also prepared by simple Fe^{3+} ion exchange with Na^+ and Ca^{2+} sites of Na-montmorillonite or by the interaction of Na-montmorillonite with the colloid in aqueous solution formed by the reaction of Fe^{3+} and NaOH (molar ratio of 1:2). The sodium content in Fe-montmorillonite (Fe 14.0 wt %) and simple Fe^{3+} ion-exchanged montmorillonite (Fe 2.8 wt %) powder was determined to be 0.173 (±0.002) and 0.188 (±0.002) wt %, respectively, by inductively coupled plasma (ICP) measurements combined with optical emission spectroscopy (Prodigy, Leeman Labs) at the Center of Advanced Materials Analysis, Tokyo Institute of Technology (Dr. T. Toya). Hence, 94.0% of Na^+ sites in Na-montmorillonite were exchanged with Fe^{3+} by simple ion exchange. An excess amount of Fe^{3+} introduced and/or the addition of NaOH to prepare Fe-

* To whom correspondence should be addressed. E-mail: yizumi@chemenv.titech.ac.jp.
† Tokyo Institute of Technology.
‡ Institute of Research and Innovation.

10.1021/jp047571o CCC: $30.25
Published on Web 01/21/2005

montmorillonite had a negligible effect on Na^+ site substitution. A high level (94.5%) of Na^+ sites at the interlayer space were effectively substituted by Fe^{3+} ions for Fe-montmorillonite (Fe 14.0 wt %).

Arsenic Adsorption Tests. A quantity (20 mL) of 0.2−16 ppm solutions of $As^{III}_2O_3$ or $KH_2As^VO_4$ was introduced to 50 mg of Fe-montmorillonites or α-FeO(OH) (Kanto Chemicals, Goethite >95.0%) in a 30-ml polypropylene tube. The mixture was shaken at a rate of 130× min^{-1} at 290 K for 12 h. The system reached an adsorption equilibrium within 12 h. The equilibrium dissolved As concentration was determined by ICP measurements.

BET Surface Area and X-ray Diffraction Measurements. The BET surface area was measured using a BELSORP 28SA (Bell Japan) with nitrogen gas as the adsorbate. The Fe-montmorillonites were evacuated at 313−423 K for 1 h before measurements. X-ray diffraction (XRD) data were obtained using a Multiflex-S diffractometer (Rigaku). Cu Kα emission was used with a Ni filter. The diffractions were monitored for Bragg angles (θ_B) between $2\theta_B = 2.0°$ and 60.0°.

Fe K-edge XAFS Measurements. The Fe-montmorillonites (0, 2.8, and 14.0 wt % Fe added) were evacuated at 290 K and transferred to a Pyrex glass cell. The windows were sealed with Kapton film of 12.5 μm thickness. α-Fe_2O_3 was mixed well with boron nitride (BN) and pressed into a disk of $\phi = 20$ mm to give an Fe K absorption edge jump value of 1.0. The Fe K-edge XAFS spectra were measured at Beamline 10B of KEK-PF in a transmission mode at 290 K. The storage ring energy was 2.5 GeV, and the ring current was 440−315 mA. A Si-(311) double crystal monochromator was used. Nitrogen gas and a mixture of N_2 (85%) and Ar (15%) gases were used in the I_0 and I_t ion chambers (Oken), respectively. The rising edge energy of the Fe metal foil was calibrated at 7111.20 eV.[6] The scan steps were ∼0.1, ∼0.5, and ∼2 eV for the edge, post-edge (XANES), and EXAFS regions, respectively. The integration time for a data point was 1−10 s.

As K-edge XAFS Measurements. As K-edge XAFS spectra were measured at 290 K for 0.13−0.48 wt % of As adsorbed onto Fe-montmorillonites at Beamline 10XU of SPring-8 by utilizing a high-energy-resolution fluorescence spectrometer.[7−9] All of the samples were pressed into a disk of $\phi = 20$ mm. Standard As samples were diluted with BN to 2.0 wt % As. The storage ring energy was 8.0 GeV, and the ring current was 97−50 mA. A Si(111) double crystal monochromator was used. A rhodium-coated double mirror set was inserted in the incident X-ray beam path at 3.0 mrad in order to suppress the higher harmonics. The undulator gap and the $\Delta\theta$ of the second crystal of the monochromator (rocking curve) were optimized to maximize the beam flux at each data scan point. The scan steps were ∼0.2, ∼0.5, and ∼2 eV for the edge, post-edge (XANES), and EXAFS regions, respectively. The integration time for a data point was 10−60 s.

The homemade high-energy-resolution Rowland-type fluorescence spectrometer selectively counts the X-ray fluorescence emitted from the sample over a small energy band (0.3−10 eV) and thus enables higher-energy-resolution XAFS spectra[7,8] and the measurement with high *S*/*B* ratio of trace amounts of elements in samples that contain high concentrations of heavy elements.[4,5] The Rowland radius was 220 mm and a Johansson-type Ge(555) crystal (Saint-Gobain) was mounted.

XAFS Data Analysis. The EXAFS data analysis was performed using XDAP (XAFS Services International) based on the works of M. Vaarkamp, H. Linders, and D. Koingsberger.

TABLE 1: Basic Physicochemical Data of Fe-Montmorillonites with the Fe Loading of 0−14.0 wt %

Fe loading[a] (wt %)	$Fe^{3+}/(Na^+ + 2Ca^{2+})$	d_{001} (Å)	specific SA ($m^2\ g^{-1}$)
0	0	12.2	25.8
2.8	0.34	12.7	45.8
7.0	1.1	13.5	66.7
14.0	2.0	15.3	100

[a] Fe included in as-received Na-montmorillonite was not counted.

The pre-edge background was approximated by the modified Victoreen function

$$\frac{C_2}{E^2} + \frac{C_1}{E} + C_0$$

The background was approximated by a smoothing spline calculated by the equation

$$\sum_{i=1}^{N} \frac{(\mu x_i - BG_i)^2}{\exp(-0.075k_i^2)} \leq \text{smoothing parameter}$$

Multiple shell analyses were performed for the Fourier-filtered EXAFS data using empirical parameters for Fe−O and Fe···Fe extracted from EXAFS for α-Fe_2O_3 and for As−O and As···Fe extracted from EXAFS for $FeAsO_4$. The bond distances and coordination numbers were based on crystal structure data for α-Fe_2O_3[10,11] and $FeAsO_4$.[12] Listed σ^2 values (Tables 2 and 3) are relative ($\Delta\sigma^2$) to those of corresponding model parameters. The goodness of fit was given as requested by the Committee on Standards and Criteria in X-ray Absorption Spectroscopy.

Results

Screening of Adsorbents among Fe^{III}-Based Materials. Screening of adsorbents among Fe^{III}-based materials was performed with 0.2−16 ppm (starting concentrations) of arsenic test solutions. The weight ratio of adsorbed As and adsorbent was optimized at the equilibrated condition (12 h). Lenoble et al.[13] and Dixit et al.[14] reported the greatest adsorption amounts of arsenite and arsenate, respectively, on α-FeO(OH) in the equilibrium dissolved As concentration range of 0.5−11 ppm (Figure 1). Data for α-FeO(OH) with a specific SA of 16 $m^2\ g^{-1}$ were added in this work. Greater As adsorption was observed as the specific SA increased, but exceptions of the correlation order were found (Figure 1A,B).

The screening using Fe^{3+} ion-exchanged montmorillonite and using montmorillonite intereacted with colloid particles formed in aqueous solution by the reaction of Fe^{3+} and NaOH was unsuccessful.[3] The weight ratio of adsorbed As and adsorbent was always smaller than the values for α-FeO(OH) with a specific SA of 54 $m^2\ g^{-1}$.[14] The screening included former adsorbents with an Fe loading of 2.8 wt % and latter adsorbents of 2.0−26.5 wt % Fe. As entirely no adsorption of As^{III}/As^V was observed on native Na-montmorillonite, Fe species were responsible for the As uptake.

In the adsorption of arsenate, the greatest weight ratio of adsorbed As and adsorbent was found on the Fe-montmorillonite (see the Experimental Section). The screening included samples of 2.8−14.0 wt % Fe. The best results were shown in Figure 1B for the sample of 14.0 wt % Fe. Because of the remarkable difference in adsorption capacity, the equilibrium dissolved As concentrations were very small for the Fe-montmorillonite. The data also fit well with a Langmuir-type equation. We did not

TABLE 2: Best-Fit Results of Fe K-edge EXAFS for Na-Montmorillonite and Fe-Montmorillonites with Fe Loadings of 2.8 and 14.0 wt %[a]

sample of fit	Fe−O				Fe···Fe				goodness of fit
R-range (Å)		(Å)	(eV)	($Å^2$)		(Å)	(eV)	($Å^2$)	
k-range ($Å^{-1}$)	N^c	*R*	ΔE_0	$\Delta\sigma^2$	N^c	*R*	ΔE_0	$\Delta\sigma^2$	
				Na-Montmorillonite					
3.3−11.0	6.0	2.122	−4.3	−0.0057					930
1.1−2.1	(±0.4)	(±0.002)	(±0.8)	(±0.0006)					
				Fe-Montmorillonites, Fe 2.8 wt %					
3.4−11.0	6.4	2.074	−0.9	−0.0019	1.4	3.269	−2.7	0.0016	113
1.1−3.0	(±1.0)	(±0.007)	(±1.3)	(±0.0009)	(±0.3)	(±0.008)	(±1.8)	(±0.0008)	
				Fe-Montmorillonites, Fe 14.0 wt %					
3.1−11.0	6.0	2.046	−0.7	0.00031	2.5	3.270	−3.1	0.00029	256
1.1−3.2	(±1.0)	(±0.009)	(±1.7)	(±0.0005)	(±0.6)	(±0.010)	(±2.2)	(±0.0002)	
α-Fe_2O_3[b]	6	2.0305			7	3.1293			
α-FeO(OH)[b]	6	2.021			2	3.015,			
					6	3.390			
γ-FeO(OH)[b]	6	2.034			6	3.066			

[a] Values in parentheses are the fit errors. [b] Based on X-ray crystallographic data in refs 10−11. [c] S_0^2 values were set to 1.

TABLE 3: Best-Fit Results of As K-edge EXAFS for As Adsorbed on Fe-Montmorillonite (Fe 14.0 wt %) from 200 ppb Test Solution of Arsenite[a]

sample of fit	As−O				As···Fe				goodness of fit
R-range (Å)		(Å)	(eV)	($Å^2$)		(Å)	(eV)	($Å^2$)	
k-range ($Å^{-1}$)	N^c	*R*	ΔE_0	$\Delta\sigma^2$	N^c	*R*	ΔE_0	$\Delta\sigma^2$	
3.9−12.0	4.2	1.679	4.8	0.0034	2.1	3.308	2.7	0.0040	456
0.9−3.2	(±0.8)	(±0.004)	(±1.6)	(±0.002)	(±0.6)	(±0.01)	(±1.1)	(±0.001)	
$FeAsO_4$[b]	4	1.6873			4	3.36			

[a] Values in parentheses are the fit errors. [b] Based on X-ray crystallographic data in ref 12. [c] S_0^2 values were set to 1.

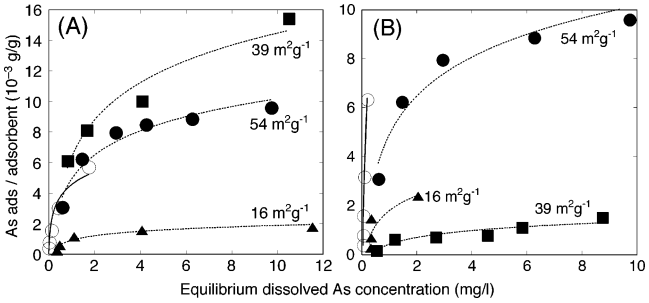

Figure 1. Adsorption isotherms of arsenite (A) and arsenate (B) at 290 K on Fe-montmorillonite (14.0 wt % Fe) (○) or α-FeO(OH) (▲, ●, and ■). Observed data were plotted as points, and the fits to first-order Langmuir-type equatios were drawn as lines. The data for α-FeO-(OH) (39 and 54 $m^2\ g^{-1}$) are from refs 13 and 14.

add the data of adsorption tests from arsenite solution in concentrations of 50−100 ppm, because 16 ppm of arsenite is near the upper limit of plausible modern environmental conditions.

In the adsorption of arsenite, the greatest weight ratio of adsorbed As and adsorbent was observed on the Fe-montmorillonite below the equilibrium dissolved As concentrations of 310 ppb, but above the As concentration, α-FeO(OH) (39 $m^2\ g^{-1}$) was the best instead (Figure 1A). This is due to a larger equilibrium adsorption constant for Fe-montmorillonite compared to that for α-FeO(OH) samples. In the practical point of view, a lower As concentration range is more important, because the application is to reduce the equilibrium dissolved As concentrations to less than 10 ppb.

Adsorbed amounts of As were also compared to the saturated adsorbed As amount per Fe amount using fits with the Langmuir-type equation. The values for As^{III} were 57 and 26 mg_{As}/g_{Fe} on Fe-montmorillonite and α-FeO(OH) (39 $m^2\ g^{-1}$), respectively. Those for As^V were 540 and 21 mg_{As}/g_{Fe} on Fe-montmorillonite and α-FeO(OH) (54 $m^2\ g^{-1}$), respectively. Thus, the practical superiority of Fe-montmorillonite is clear. Preliminary adsorption tests of arsenic on Ti, Mn, Co, Ni, Zn, Zr, Nb, or Mo intercalated between montmorillonites were also performed. The saturated adsorbed amounts of As^{III}/As^V were greatest in the case where Fe was intercalated.

In summary, the Fe-montmorillonite (14.0 wt % Fe) was the best adsorbent for low concentrations of both arsenite and arsenate (<310 ppb) on the basis of the screening tests among the Fe^{III}-based materials.

Basic Physicochemical Characterization of Fe-Montmorillonites. Basic physicochemical data for the Fe-montmorillonites were summarized in Table 1. The maximum loading of Fe was 14 wt %. Excessive Fe greater than 14.0 wt % was eluted by washing with distilled water during the sample preparation. Fe (2.8 wt %) corresponds to the maximum ion-exchangeable Fe^{3+} amount replacing Na^+ and Ca^{2+} sites of Na-montmorillonite, with each charge taken into account (Table 1).

On the basis of the strongest peak angles due to (001) diffraction (and also the relatively weaker (002) diffraction peak) in the XRD spectra, interlayer spacings of montmorillonite were monitored. The interlayer spacings and specific SA gradually increased starting from 12.2 Å and 25.8 $m^2\ g^{-1}$ (Na-montmorillonite) to 15.3 Å and 100 $m^2\ g^{-1}$ (Fe-montmorillonite, 14.0 wt % Fe), respectively (Table 1). These data demonstrate that the intercalated Fe^{III} species increased the interlayer spacings and the clearance for N_2 molecules.

Fe K-edge EXAFS. The structure of intercalated Fe^{III} species was studied by Fe K-edge EXAFS. The EXAFS spectra of Na-montmorillonite (one montmorillonite layer consists of three sheets, and 1.55 wt % of Fe is contained in the middle sheet[15]) and Fe-montmorillonites (Fe 2.8 and 14.0 wt %) were studied (Table 2).

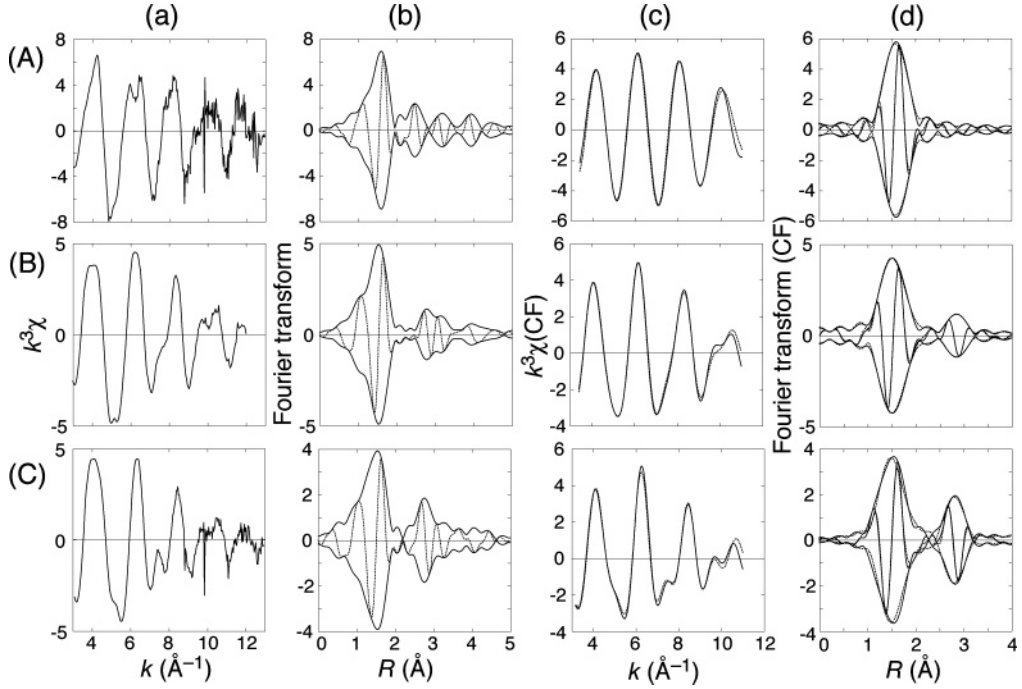

Figure 2. Fe K-edge EXAFS spectrum measured at 290 K for Na-montmorillonite (A) and Fe-montmorillonites (Fe 2.8 wt % (B) and 14.0 wt % (C)). (a) k^3-weighted EXAFS χ function, (b) its associated Fourier transform (—, magnitude; ···, imaginary part), and curve-fitting analysis to the inversely Fourier-filtered $k^3\chi$ function in k-space (c) and in R-space (d) (—, experimental; ···, calculated).

The Fourier transforms are depicted in Figure 2b. Although the strongest peak at 1.6 Å (phase-shift uncorrected) was common for the three samples studied (A−C), the next-nearest peak appeared at 2.5 Å (phase-shift uncorrected) for Na-montmorillonite (A−b), shorter than 2.8 Å (phase-shift uncorrected) for Fe-montmorillonites (B−b and C−b). Thus, the major backstattering atoms are Si and Al for Na-montmorillonite[15] and Fe for Fe-montmorillonites.

Best-fit results are listed in Table 2. The coordination number (N) of Fe−O was 6.0 for Na-montmorillonite, consistent with the octahedral symmetry in the middle sheet of the montmorillonite layer.[15] Obtained N values of Fe−O were 6.0−6.4 for Fe-montmorillonites. [FeO_6] units were suggested. The Fe−O distances for Fe-montmorillonites (2.8−14.0 wt % Fe) were 2.046−2.074 Å, relaxed from 2.021 Å for α-FeO(OH) and 2.034 Å for γ-FeO(OH) (Table 2). The obtained Fe···Fe distance was essentially constant (3.269−3.270 Å) for Fe-montmorillonites (Table 2). This Fe···Fe distance is within the range for edge-shared [FeO_6] octahedral structure (2.97−3.28 Å).[16] The N values obtained for Fe···Fe were 1.4−2.5.

In a similar preparation route of Fe-montmorillonite but in the absence of NaOH (the molar ratio of Fe^{3+}/NaOH was 1:2 in our study), an intercalated $Fe(OH)_2$-like sheet structure was proposed.[17] The alkaline addition may have the effect of growing the Fe species to nanoparticles between layers. When our Fe-montmorillonite sample (Fe 14.0 wt %) was heated at 623 K in a vacuum, the XANES pattern and EXAFS data (not shown) became similar to those of α-Fe_2O_3. Thus, nonheated Fe-montmorillonites studied in Table 2 are suggested to be FeO(OH)-like nanoparticles.

In summary, intercalated FeO(OH) particles of Fe-montmorillonite (14.0 wt % Fe) consisted of edge-shared [FeO_6] octahedral units. The size was limited on the basis of N for Fe···Fe (2.5), consistent with the d_{001} value increase by 3.1 Å compared to that for Na-montmorillonite (Table 1). The octahedral structure was relaxed compared to the units in α-FeO(OH) or γ-FeO(OH) crystals.

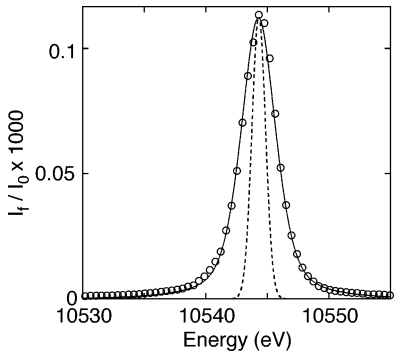

Figure 3. As Kα$_1$ emission spectrum for As adsorbed on Fe-montmorillonite (14.0 wt % Fe) from 200 ppb test solution of arsenite (points). A fit to data with pseudo-Voigt function (—) and the energy resolution of the fluorescence spectrometer (···) were also drawn.

As K-edge XANES Combined with Fluorescence Spectrometry. The As Kα$_1$ emission peaks for the As adsorbed on Fe-montmorillonite (14.0 wt % Fe) from 0.2 to 16 ppm of arsenite solutions always appeared at 0.6 eV higher than that for As metal (Figure 3). The chemical shifts of the As Kα$_1$ peak were −1.4 and +0.6 eV for As_2O_3 and KH_2AsO_4, respectively, with reference to As metal. The fwhm (full width at half-maximum) of the observed peak was 3.36 eV (Figure 3). Because the lifetime width of As Kα$_1$ is 3.08 eV,[18] the energy resolution of this fluorescence spectrometer was estimated to be 1.3 eV (···, Figure 3), including the contribution of the beamline. Because the energy resolution value was smaller than the core-hole lifetime width of As K-level (2.15 eV),[18] the lifetime broadening should be removed at the As K-edge.[7,8,19,20]

The fluorescence spectrometer was tuned to 10 544.3 eV (peak top). Then, XANES spectra were measured using high-energy-resolution X-ray fluorescence spectrometry for As adsorbed on Fe-montmorillonites (Figure 4d−f). Note that spectra a−c were measured in transmission mode, and the peaks were broader compared to those in spectra d−f. The white line peak

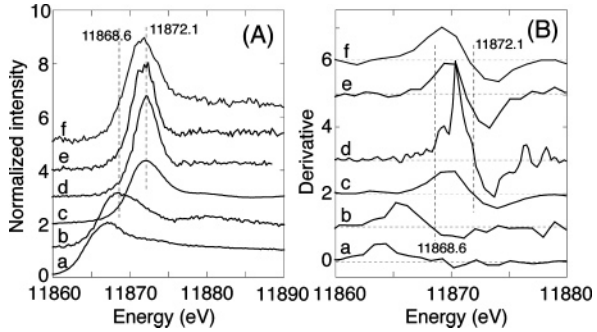

Figure 4. (A) Normalized As K-edge XANES spectra combined with fluorescence spectrometry at 290 K for As adsorbed on Fe-montmorillonite (14.0 wt % Fe) (d−f) from aqueous test solutions of 16 ppm of KH_2AsO_4 (d), 16 ppm of As_2O_3 (e), and 200 ppb of As_2O_3 (f). Reference XANES spectra measured in transmission mode for As metal (a), As_2O_3 (b), and KH_2AsO_4 (c). (B) First derivative spectra of (A).

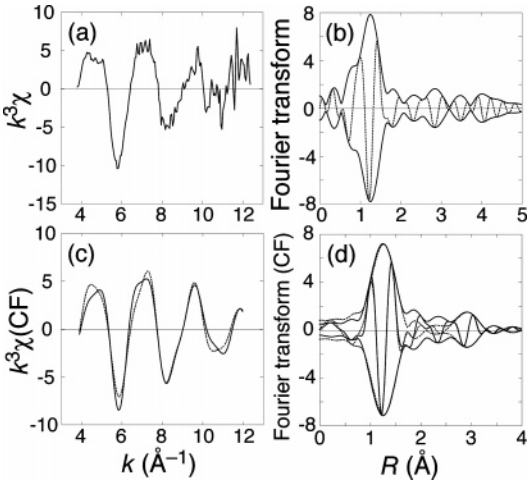

Figure 5. As K-edge EXAFS spectrum measured at 290 K for As on Fe-montmorillonite from 200 ppb test solution of arsenite. (a) k^3-weighted EXAFS χ function, (b) its associated Fourier transform (—, magnitude; ···, imaginary part), and curve-fitting analysis to the inversely Fourier-filtered $k^3\chi$ function in k-space (c) and in R-space (d) (—, experimental; ···, calculated).

for As adsorbed from 16 ppm test solution of arsenate appeared at 11 872.1 eV (d), at the identical energy as KH_2AsO_4 (c).

The white line peak for As adsorbed from 0.2 to 16 ppm test solutions of arsenite appeared at 11 871.7−11 871.9 eV (e and f), very near to the peak for KH_2AsO_4 (c) rather than As_2O_3 (b, 11 868.6 eV). The peaks were not symmetrical. These comparisons of peak energy position were carefully checked for the first derivative spectra (Figure 4B).

In summary, the speciation of As was successfully performed by the chemical shifts of the As Kα_1 peak and the energy shifts of the white line in the As K-edge XANES. A major part of arsenite was oxidized to arsenate upon the adsorption on the Fe-montmorillonite from 0.2 to 16 ppm test solutions. This oxidation was not observed in the adsorption from 50 to 100 ppm of arsenite test solutions.

As K-edge EXAFS. The adsorbed state of As from a 200 ppb test solution of arsenite was studied using As K-edge EXAFS (Figure 5 and Table 3). The As−O distance obtained was 1.679 Å. These data supported the oxidative adsorption of arsenite. As−O bond distances of 1.78−1.79 and 1.69 Å have been reported for As^{III} [21,22] and As^{V} species,[21] respectively, adsorbed on γ-FeO(OH) and α-FeO(OH).

A weak peak appeared at 2.8 Å (phase shift uncorrected) in the Fourier transform (Figure 5b). The peak was fit as an As···Fe bond of 3.308 Å with an N value of 2.1 (Table 3). The As···Fe distances have been reported as 3.6, 3.24−3.32, and 2.83−2.85 Å for monodentate mononuclear, bidentate binuclear (bridging), and bidentate mononuclear As^{V} complexes, respectively,[11,21−24] and 3.36−3.40 Å for bidentate binuclear As^{III} species on Fe oxyhydroxides.[22] The As···Fe distance obtained in this work corresponds to the bidentate binuclear As^{V}: the arsenate being connected to the adjacent apexes of edge-sharing [FeO_6] units.

Discussion

By the screening tests of Fe^{III}-based adsorbents with 0.2−16 ppm test solutions of arsenite/arsenate, the Fe-montmorillonite (14.0 wt % Fe added) was found to be the best (Figure 1). As a general trend, the weight ratio of adsorbed As and adsorbent increased as the specific SA of adsorbent grew greater (Table 1 and Figure 1). The specific SA for Fe-montmorillonite (14.0 wt % Fe) was 100 $m^2\ g^{-1}$.

The trend of adsorption isotherms between arsenite and arsenate adsorptions was in good contrast (Figure 1). The Fe-montmorillonite (14.0 wt % Fe) was found to be best for arsenite adsorption capacity in the equilibrium dissolved As concentration smaller than 310 ppb, in contrast to the dramatic improvement of arsenate adsorption capacity in the entire As concentration range studied. In the As adsorption conditions of this study, arsenite and arsenate are dissolved in water as $As^{III}(OH)_3$ and $[As^{V}O_2(OH)_2]^-$, respectively.[25] The charge of As molecules may affect the complex formation with the surface of FeO(OH).

The thickness of one layer of montmorillonite is ∼9.3 Å.[24] Therefore, the average interlayer clearance is estimated to 6.0 Å for Fe-montmorillonite (Fe 14.0 wt %, Table 1). On the basis of the Fe K-edge EXAFS, the structural unit of edge-shared [FeO_6] was suggested for the adsorbent. Because the Fe···Fe distance obtained (3.270 Å, Table 2) was more than the half of 6.0 Å, the interconnection of [FeO_6] units should be in the direction (nearly) parallel to the layers. The N value for Fe···Fe (2.5) suggested a limited number of interconnections of [FeO_6] units. It is important to note that the Fe K-edge EXAFS data for the Fe-montmorillonites exhibited negligible change after the As adsorption tests (Figure 1) compared to data obtained prior to the tests (Figure 2B,C). The montmorillonite swells up in aqueous solution, and the FeO(OH) particles may not be closely packed between layers during adsorption tests of As. Hence, the performance observed in Figure 1 is primarily due to the unsaturated nature of the very small Fe^{III} particle size and not a geometric effect between packed layers.

On the basis of the As K-edge XANES combined with fluorescence spectrometry (Figure 4), oxidative adsorption of arsenite was observed on Fe-montmorillonite (14.0 wt % Fe) from 0.2 to 16 ppm test solutions. The energy levels at which the derivative XANES data cross the line of $y = 0$ for the standards of As^{III} and As^{V} were 11 868.6 and 11 872.1 eV, respectively (Figure 4B, b and c). Corresponding values for adsorbed As derived from As_2O_3 were 11 871.3 (e) and 11 871.6 eV (f). If a linear combination of As^{III} and As^{V} peaks is assumed, the population of As species that converted from arsenite to arsenate upon adsorption was estimated to be 77% and 85%, respectively. Note that this estimation was improved when combined with high-energy-resolution fluorescence spectrometry by the removal of lifetime broadening.[7,8,19,20] The white line peaks for d−f utilizing fluorescence spectrometry were sharper compared to spectra a−c obtained in the transmission mode. This finding of oxidative adsorption of arsenite was supported

by the chemical shifts of As Kα_1 emission spectra (Figure 3) and As−O and As···Fe bond distances obtained by As K-edge EXAFS (1.679 and 3.308 Å, respectively; Table 3). The surface As complex was suggested to be bidentate binuclear As^V species.[11,21−24] The fit values may not be exact, because ∼15% of As^{III} coexisted on the basis of As K-edge XANES (Figure 4f).

Homogeneous oxidation of a 30 ppm arsenite solution was reported at pH greater than 9.[26] The pH in the arsenite adsorption of this study (Figure 1A) was 6.0−3.9, and the possibility of homogeneous oxidation of arsenite is rejected. No oxidation upon adsorption was reported for 6.0−15 ppm test solutions of arsenite on α-FeO(OH) and γ-FeO(OH).[21] Thus, the smaller particle size of FeO(OH) on the scale of 6 Å, and accordingly higher population of the adjacent apexes of edge-sharing [FeO_6] units, may be the primary reason of the greatest As adsorption capacity (Figure 1) among Fe^{III}-based materials.

As observed in Figure 1, it is a general trend that arsenate uptake is several times greater than that of arsenite on Fe^{III}-based materials except for α-FeO(OH) (39 m^2 g^{-1}). In this context, one of the reasons for superior arsenite uptake on Fe-montmorillonite at lower As concentrations is its oxidation to arsenate upon adsorption. Final adsorbed As local structures from 0.2 to 16 ppm test solutions were very similar either from arsenite and arsenate (Table 3 and Figures 4 and 5). The responsible sites on FeO(OH) nanoparticles may work as $As^{III}(OH)_3$ + FeO(OH)(surface) → $As^V(OH)_2O_2Fe$(surface) + H_2O. Two prerequisites, this oxidation step and a higher population of coordinatively unsaturated sites on FeO(OH), may determine the uptake amonts of arsenite on Fe-montmorillonites. The Fe K-edge shift was studied for Fe-montmorillonite in 16 ppm of arsenite test solution (Figure 1). No change was observed at the edge upon adsorption of As, because the molar ratio of adorbed As and Fe was only 0.031.

Conclusions

Among Fe^{III}-based materials studied and in the literature, intercalated Fe-montmorillonites prepared in this work exhibited the best arsenate adsorption capacity on an adsorbent weight basis from 0.2 to 16 ppm test solutions. The adsorbents were also best for arsenite sorption capacity below the equilibrium dissolved As concentrations of 310 ppb.

The structure of responsible Fe^{III} sites was studied for optimized Fe-montmorillonite (14.0 wt % Fe). The size of intercalated FeO(OH) particles was 6.0 Å in the direction perpendicular to montmorillonite layers based on XRD. The information for Fe−O at 2.046 Å and Fe···Fe bonds at 3.270 Å by Fe K-edge EXAFS demonstrated octahedral [FeO_6] units interconnected in the direction (nearly) parallel to the layers. The number of units per particle should be very limited.

The speciation of As adsorbed on the Fe-montmorillonite (14.0 wt % Fe) was performed by As K-edge XAFS combined with high-energy-resolution fluorescence spectrometry. The technique removed lifetime broadening and thus enabled one to quantitatively monitor the oxidative adsorption of a major part (77−85%) of arsenite to arsenate from 0.2 to 16 ppm test solutions. This finding was supported by the chemical shifts of As Kα_1 emission peaks and the information for As−O at 1.679 Å and As···Fe bonds at 3.308 Å by As K-edge EXAFS.

The greatest As sorption capacity per adsorbent weight for Fe-montmorillonite may be due to the metric size (6 Å) of intercalated FeO(OH) particles and accordingly higher populations of the adjacent apexes of edge-shareing [FeO_6] units.

Acknowledgment. The XAFS experiments were performed under the approval of the SPring-8 Program Review Committee (2002B0738-NX-np, 2003A0145-NX-np) at As K-edge and under the approval of the Photon Factory Proposal Review Committee (2001G092, 2003G074) at Fe K-edge. The authors are thankful for a grant from the Grant-in-Aid for Encouragement of Young Scientists from the Ministry of Education, Culture, Sports, Science, and Technology (Y.I., 1474 0401).

References and Notes

(1) Smith, A. H.; Lopipero, P. A.; Bates, M. N.; Steinmaus, C. M. *Science* **2002**, *296*, 2145−2146.
(2) Nordstrom, D. K. *Science* **2002**, *296*, 2143−2145.
(3) Masih, D.; Seida, Y.; Izumi, Y. In preparation.
(4) Izumi, Y.; Kiyotaki, F.; Minato, T.; Seida, Y. *Anal. Chem.* **2002**, *74*, 3819−3823.
(5) Izumi, Y.; Kiyotaki, F.; Seida, Y. *J. Phys. Chem. B* **2002**, *106*, 1518−1520.
(6) Bearden, J. A. *Rev. Mod. Phys.* **1967**, *39*, 78−124.
(7) Izumi, Y.; Kiyotaki, F.; Nagamori, H.; Minato, T. *J. Electron Spectrosc. Relat. Phenom.* **2001**, *119*, 193−199.
(8) Izumi, Y.; Nagamori, H. *Bull. Chem. Soc. Jpn.* **2000**, *73*, 1581−1587.
(9) Izumi, Y.; Oyanagi, H.; Nagamori, H. *Bull. Chem. Soc. Jpn.* **2000**, *73*, 2017−2023.
(10) Blake, R. L.; Hessevick, R. E. *Am. Mineral.* **1966**, *51*, 123−129.
(11) Waychunas, G. A.; Fuller, C. C.; Rea, B. A.; Davis, J. A. *Geochim. Cosmochim. Acta* **1996**, *60*, 1765−1781.
(12) Cheetham, A. K.; David, W. I. F.; Eddy, M. M.; Jakeman, R. J. B.; Johnson, M. W.; Torardi, C. C. *Nature* **1986**, *320*, 46−48.
(13) Lenoble, V.; Bouras, O.; Deluchat, V.; Serpaud, B.; Bollinger, J. C. *J. Colloid Interface Sci.* **2002**, *255*, 52−58.
(14) Dixit, S.; Hering, J. G. *Environ. Sci. Technol.* **2003**, *37*, 4182−4189.
(15) Grim, R. E. *Clay Mineralogy*, 2nd ed.; McGraw-Hill: New York, 1968.
(16) Cornell, R. M.; Schwertmann, U. *The Iron Oxides—Structure, Properties, Reactions, Occurrence and Uses*; VCH Publishers: Weinheim, 1996; pp 12−26.
(17) Ebitani, K.; Ide, M.; Mitsudome, T.; Mizugaki, T.; Kaneda, K. *Chem. Commun.* **2002**, 690−691.
(18) Krause, M. O.; Oliver, J. H. *J. Phys. Chem. Ref. Data* **1979**, *8*, 329−338.
(19) Stojanoff, V.; Hamalainen, K.; Siddons, D. P.; Hastings, J. B.; Berman, L. E.; Cramer, S.; Smith, G. *Rev. Sci. Instrum.* **1992**, *63*, 1125−1127.
(20) Hamalainen, K.; Siddons, D. P.; Hastings, J. B.; Berman, L. E. *Phys. Rev. Lett.* **1991**, *67*, 2850−2853.
(21) Farquhar, M. L.; Charnock, J. M.; Livens, F. R.; Vaughan, D. J. *Environ. Sci. Technol.* **2002**, *36*, 1757−1762.
(22) Manning, B. A.; Fendorf, S. E.; Goldberg, S. *Environ. Sci. Technol.* **1998**, *32*, 2383−2388.
(23) Randall, S. R.; Sherman, D. M.; Ragnarsdottir, K. V. *Geochim. Cosmochim. Acta* **2001**, *65*, 1015−1023.
(24) Ladeira, A. C. Q.; Ciminelli, V. S. T.; Duarte, H. A.; Alves, M. C. M.; Ramos, A. Y. *Geochim. Cosmochim. Acta* **2001**, *65*, 1211−1217.
(25) Munoz, J. A.; Gonzalo, A.; Valiente, M. *Environ. Sci. Technol.* **2002**, *36*, 3405−3411.
(26) Manning B. A.; Goldberg, S. *Environ. Sci. Technol.* **1997**, *31*, 2005−2011.